Stem Cell Reports, Volume *11*

Supplemental Information

Defining Lineage-Specific Membrane Fluidity Signatures that Regulate Adhesion Kinetics

Takahisa Matsuzaki, Shinya Matsumoto, Toshiharu Kasai, Emi Yoshizawa, Satoshi Okamoto, Hiroshi Y. Yoshikawa, Hideki Taniguchi, and Takanori Takebe

SUPPRIMENTAL FIGURES AND LEGENDS

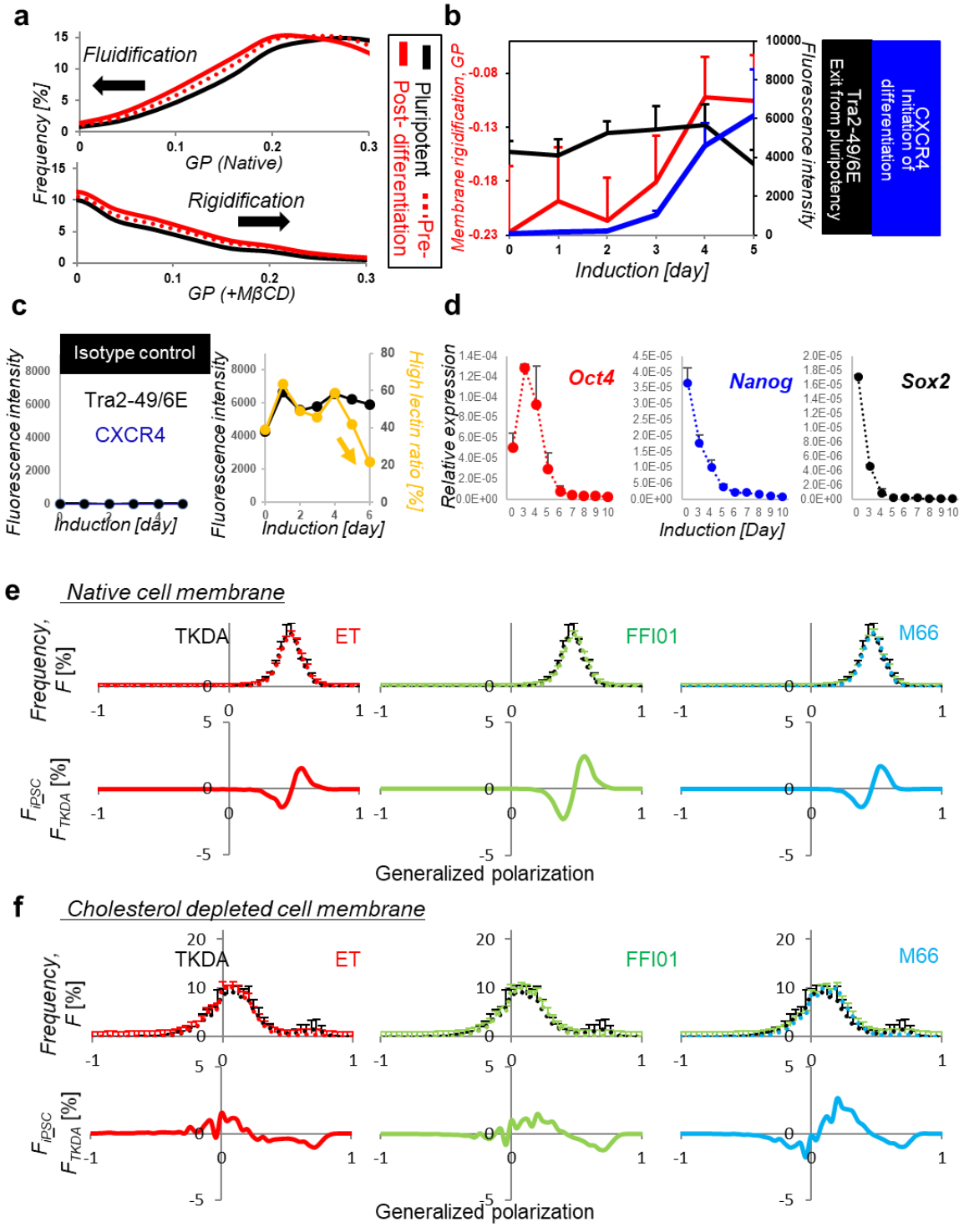

Fig. S1: Membrane rigidification precedes pluripotency exit and differentiation initiation. (a) Original fluidity histogram of pluripotent cells

during endodermal induction in the absence/presence of MβCD. (b) Summary of the statistical analysis of GP in the presence of MβCD (red, Fig. 1d) and the mean intensity of Tra2-49/6E (black) and CXCR4 (blue). It should be noted that membrane rigidification preceded (day 2), rather than followed, the exit from pluripotency (day 4) and initiation of differentiation (day 3). Three independent experiment were performed (n = 3). (c) Corresponding isotype control assessment. For all of the conditions, the background intensity was extremely low (left). The exit from pluripotency of the iPSCs after membrane rigidification was also confirmed by the addition of rBC2LCN-FITC (Wako, Japan, (Tateno et al., 2011)). The high lectin ratio (intensity level > 3×10^3 corresponding peak in the histogram) decreased from day 5 (right). (d) qPCR analysis of representative pluripotency marker (Oct4, Nanog, Sox2) for pluripotent cells during endodermal induction. Such decrease in transcriptional marker of pluripotent cells was also quantified in our previous paper (Takebe et al., 2017). Abrupt GP decrease by MβCD is not influenced by the iPSC donor differences. Raw GP histograms of iPSCs of four different donors (TKDA (dotted), ET, FFI01, M66) in the (e) absence and (f) presence of MβCD. All of the donors show a significant decrease in GP toward fluidization (left side). It should be noted that there is no significant difference between iPSC donors (except for TKDA).

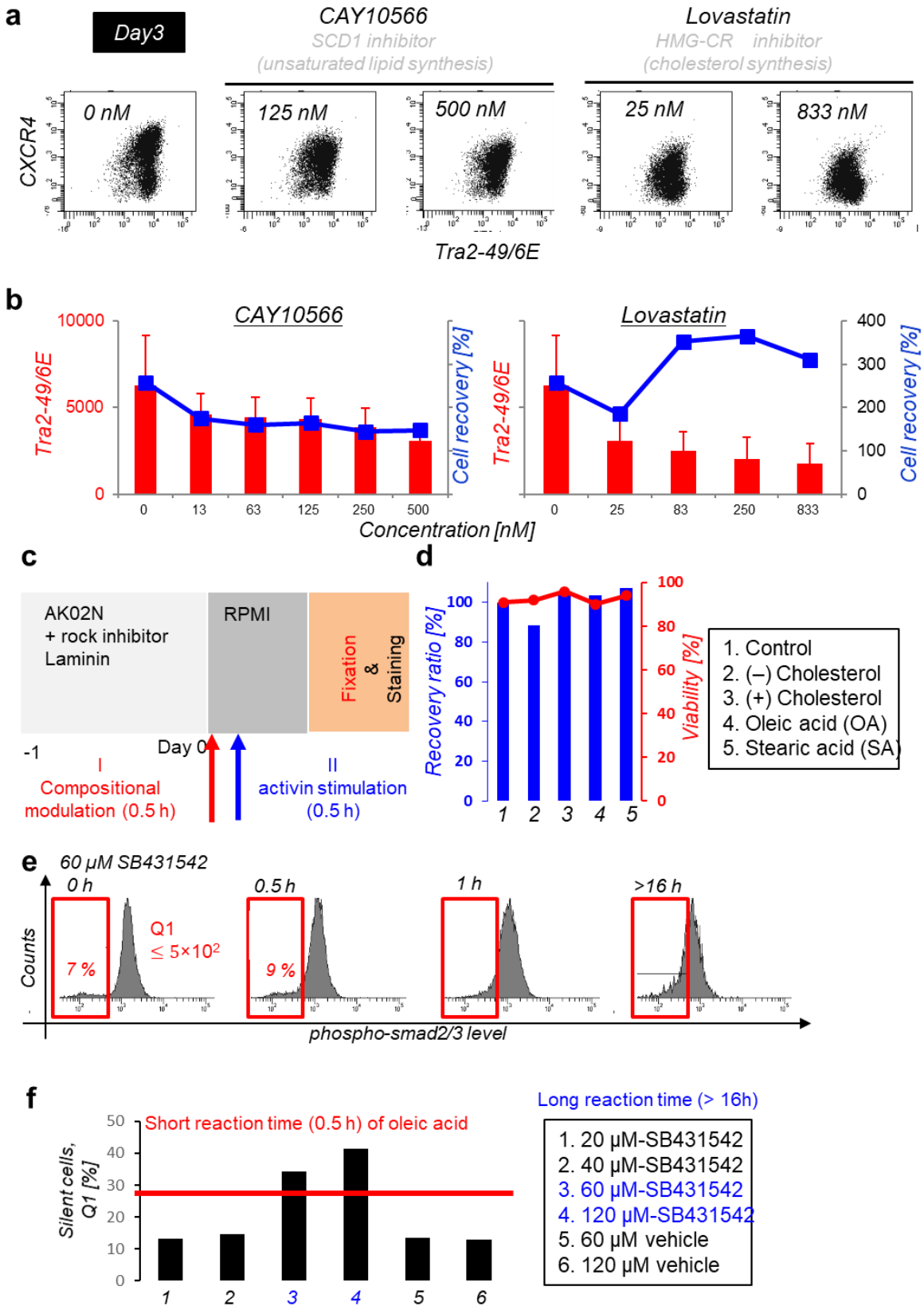

Fig. S2: Viability of differentiated cells is not significantly influenced by the inhibitors and fluidic modulator (Extended data of Fig.1g and f) (a)

Flow cytometry analysis of pluripotent cell during endodermal induction in the absence and presence of inhibitors (CAY10566 and Lovastatin). A differentiation marker (CXCR4, marker of definitive endoderm cells, DE cells, vertical) and a pluripotent marker (Tra2-49/6E, horizontal) were used. (b) Mean intensity of Tra2-49/E (vertical, left) and the cell recovery ratio (vertical, right) were co-plotted as concentration of inhibitors. Recovery ratio was calculated by the (collected cells / initial cells × 100) [%]. iPSCs were seeded (2×10^5) in the presence of 10 μM rock inhibitor (day 0) and subsequently exposed to induction medium with CAY10566/lovastatin until flow cytometry analysis (3 day). Error bars represent the standard deviations of the Tra2-49/6E histograms. (c) Detailed protocols for the fluidic modulation experiment and the (d) viability assay of the iPSC in the presence and absence of fluidic modulators (cholesterol, oleic acid, stearic acid). For the addition/depletion of cholesterol, 5 mM MβCD (+/-) cholesterol were prepared (Yamamoto et al., *J. Cell Sci.* 2012). Oleic and stearic acid were prepared onto the bovine serum albumin (900 μM in final, Briaud et al., Diabetes 2001) were used. (e) Time course of p-Smad2/3 levels in the presence of the corresponding inhibitors (SB431542). Silent cells were defined by low intensity levels (~ background, $< 5 \times 10^2$, Q1). (f) Silent cell ratios with different concentrations of SB431542. Only conditions 3 and 4 (16 h reaction) yielded a high ratio of silent cells which is comparable to the oleic

acid reaction at 30 min. For the evaluation of p-smad2/2 levels inside the cells, we followed established protocols using BD staining kit (562586, BD, Japan).

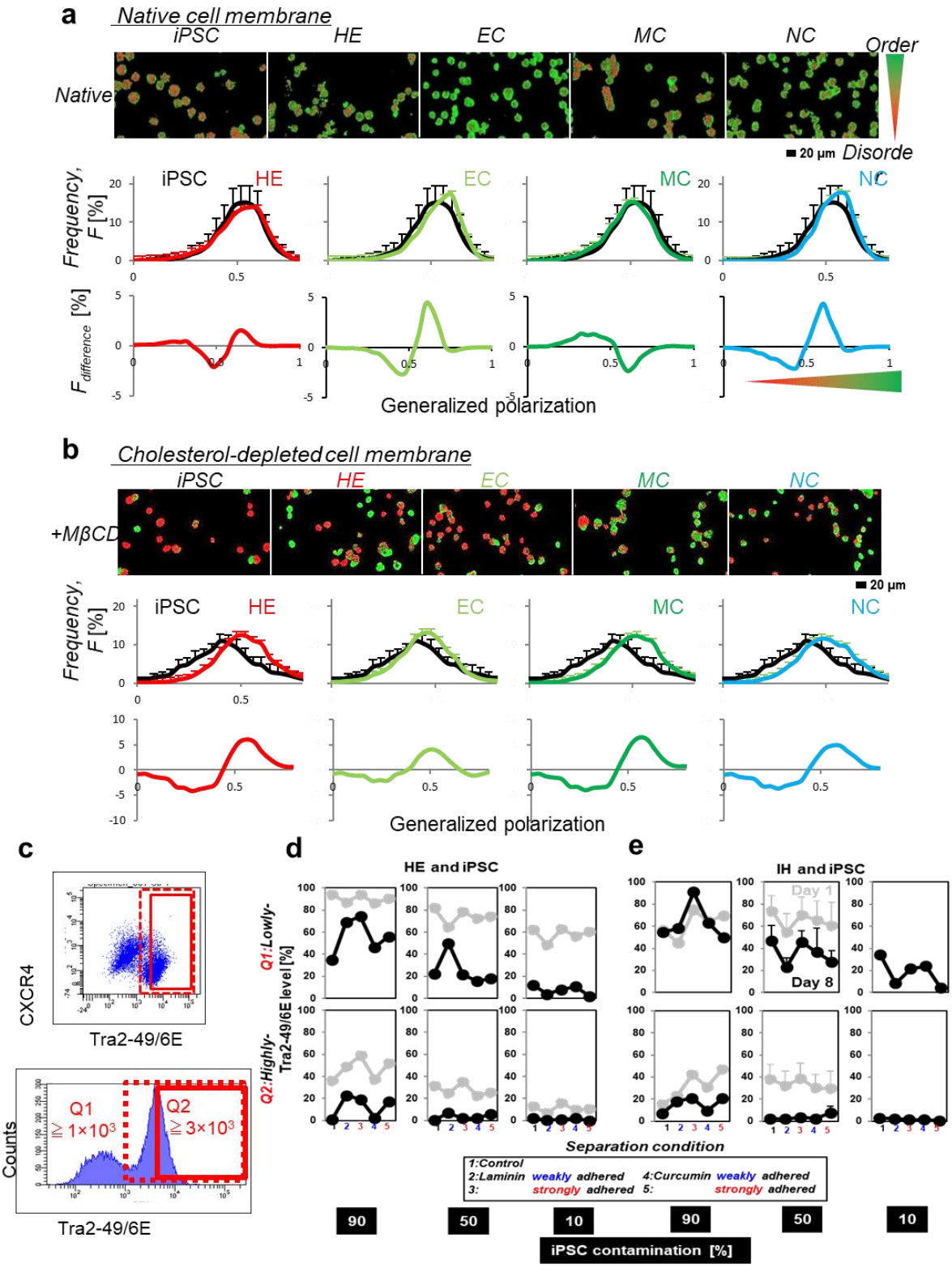

Fig. S3: Original histograms of Fig. 2b and analytical procedures for Fig.4c.

Original fluidity histogram of pluripotent cells and early differentiated progeny in the (a) absence and (b) presence of MβCD. Higher GP represents highly ordered

membrane. Subtracted histogram of $F_{difference}$ between pluripotent cells ($F_{pluripotent}$) and early differentiated progeny ($F_{differentiated}$) showed a different shape, supporting the presence of membrane fluidity signatures. Three independent experiments were performed (n = 3). (c) Detailed gating procedure for the definition of lowly/highly tra2-49/6E expressed cells. Lowly/highly tra2-49/6E expressed cells ration with different iPSC contamination levels for case of (d) HE and (e) immatured hepatocyte (IH, day 14 endodermal induction from iPSC).

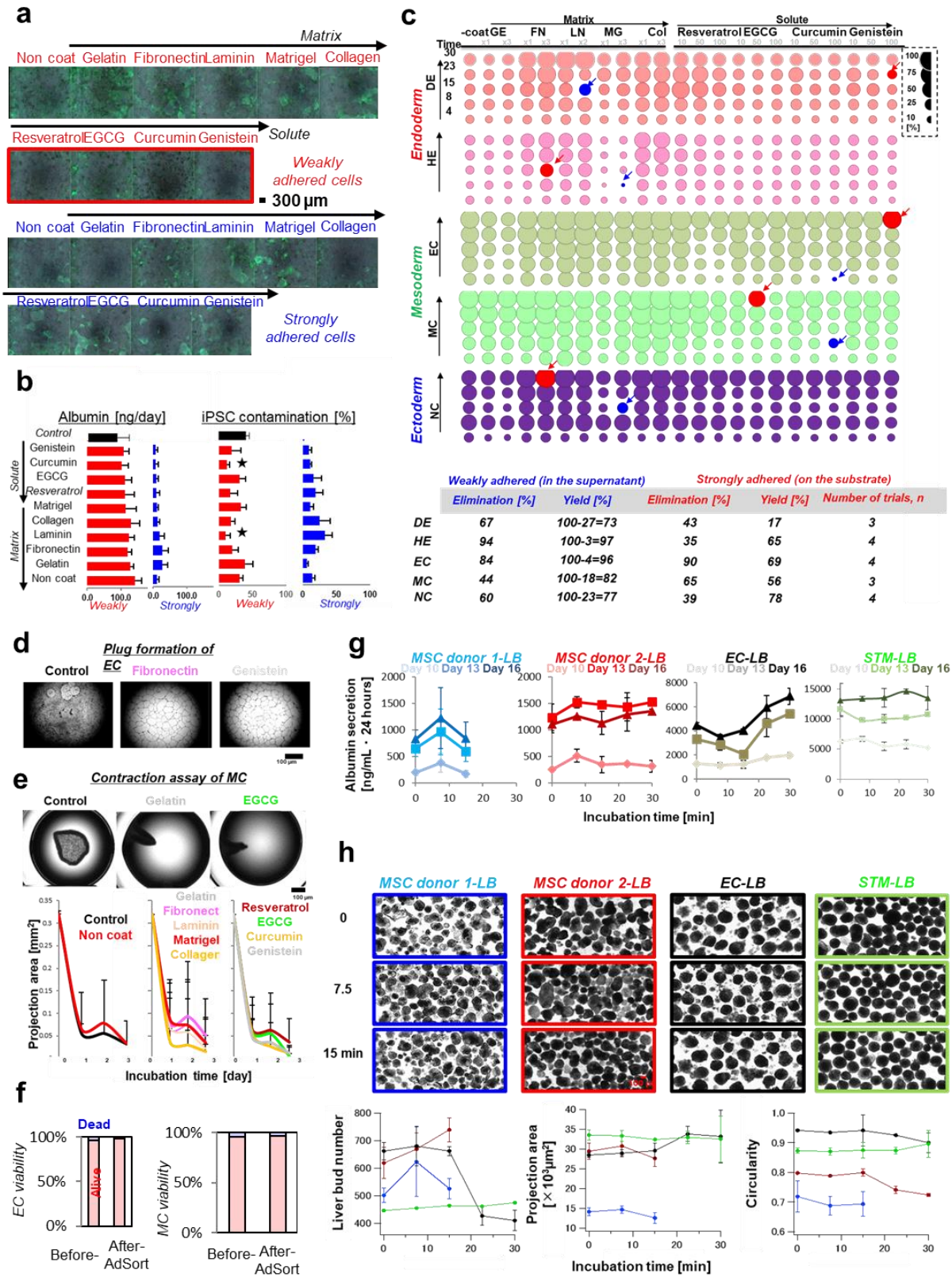

Fig. S4: Cell purification of various differentiated progeny using AdSort method. (a) Complementary experiment of iPSC (GFP-labeled) contamination after

the cell separation and the (b) statistical analysis of iPSC area. Left data is also shown in the Fig. 4c left for the reader guidance. Yield calculation for our method. (c) Adhesion ratio of the cells with different adhesion-modulating factors and the calculated yield of the cells under the maximized conditions (arrowed in the figure) with the number of trials. Separation time was set to 30 min (Fig. 4c). Resultant pluripotent level of separated hepatic endoderm was minimal level with high yield (~80 %) indicating the effective iPS elimination. Functional and viable cell purification of ECs and MCs. Semi-quantitative cell functional assay of (d) ECs and (e) MCs. Strongly adhered cells were separated as a same combination of polyphenols and matrix in Fig. 4c. Plug assay and contraction assay were performed according to the established protocols (Takebe et al., 2013). Strongly adhered cells were collected as follows: after incubation of the cells in the various culturing condition, the supernatant was aspirated and incubated with PBS with 0.8 mM EDTA for 30 min at 37 °C. The mild treatment accelerated the detachment of cells with the gentle pipetting. (f) To confirm the viability of separated cells, the strongly adhered cells after plating the cells (t= 30 min) were stained with 0.4 % trypan blue and the dead cells were counted by Countess (Invitrogen, Tokyo, Japan). Cell purification directing the functional liver bud. (g) Function and (h) morphology of liver buds (LBs) using separated supportive cells (*i.e.*, mesenchymal and endothelial cells) with following composition: MSC

donor1-LB(HE: HUVEC : MSC = 10 : 7 : 1), MSC donor2-LB(HE: HUVEC : MSC = 10 : 7 : 1), EC-LB (HE : EC = 10 : 7), and STM-LB (HE : STM = 10 : 1). Cell mixture (3×10^5 in total) were seeded in 24 well-Elplasia plate (kuraray, Japan) and exposed to hepatic differentiation medium according to the established protocols (Takebe et al., 2017).It should be noted that strongly adhere cells were used in the whole condition. We obtained umbilical cord samples following the approved guidelines set by the ethical committee at Yokohama City University (approval no. 13120510008). HUVECs and MSCs were isolated from umbilical cord as previously described (Takebe et al., 2013).

REFERENCES

Takebe, T., Sekine, K., Enomura, M., Koike, H., Kimura, M., Ogaeri, T., Zhang, R.R., Ueno, Y., Zheng, Y.W., Koike, N.*, et al.* (2013). Vascularized and functional human liver from an iPSC-derived organ bud transplant. Nature *499*, 481-484.

Takebe, T., Sekine, K., Kimura, M., Yoshizawa, E., Ayano, S., Koido, M., Funayama, S., Nakanishi, N., Hisai, T., Kobayashi, T.*, et al.* (2017). Massive and Reproducible Production of Liver Buds Entirely from Human Pluripotent Stem Cells. Cell Rep *21*, 2661-2670.

Tateno, H., Toyota, M., Saito, S., Onuma, Y., Ito, Y., Hiemori, K., Fukumura, M., Matsushima, A., Nakanishi, M., Ohnuma, K.*, et al.* (2011). Glycome diagnosis of human induced pluripotent stem cells using lectin microarray. J Biol Chem *286*, 20345-20353.